Classical Double Inverted Pendulum – a Complex Overview of a System

S. Jadlovská* and J. Sarnovský*
* Department of Cybernetics and Artificial Intelligence, Faculty of Electrical Engineering and Informatics, Technical University of Košice, Košice, Slovak Republic
e-mail: slavka.jadlovska@tuke.sk, jan.sarnovsky@tuke.sk

***Abstract*— The purpose of this article is to perform an in-depth analysis of the classical double inverted pendulum system using the *Inverted Pendula Modeling and Control* (*IPMaC*), a *Simulink* block library designed by the authors of the paper. The custom function blocks included in the *IPMaC* offer comprehensive program support for the modeling, simulation and control of classical and rotary inverted pendula systems. The library also incorporates software tools which provide a user-friendly graphical interface (GUI) to modeling and linearization procedures. With the aid of appropriate function blocks, GUI tools and demonstration schemes from the *IPMaC*, the classical double inverted pendulum system is analyzed, modeled and successfully stabilized in the unstable inverted position.**

I. Introduction

Inverted pendula systems represent a significant class of highly nonlinear mechanical systems used in classical control education. Practical problems which can be simulated by some kind of an inverted pendula system include balancing a broomstick on a handpalm, stabilization of a walking human or robot, control of a launching rocket or the vertical movement of a human shoulder or arm [1][2]. The diversity of modeled systems is reflected in the wide variety of available inverted pendula models. Hence we can distinguish between:

- inverted pendula systems with a base that moves in a linear manner (*classical inverted pendula systems*) or in a rotary manner in a horizontal plane (*rotary inverted pendula systems*)
- *single*, *double*, *triple* or *quadruple* inverted pendula systems, which differ by the number of pendulum links attached to the base.

As an underactuated, extremely unstable and yet controllable system, the classical double (two-link) inverted pendulum has become an attractive testbed system for linear and nonlinear control law verification ever since it was introduced to feedback control community. This paper will present a overview of this popular system, covering every significant step from mathematical model derivation to examples of control algorithm design. The individual steps of the process will be demonstrated using suitable function blocks or GUI applications from the *Inverted Pendula Modeling and Control (IPMaC)* block library. The *IPMaC* was developed between 2009-11 by the authors of this paper as a thematic Simulink library in order to provide software support for the analysis and control of classical and rotary inverted pendula systems [1][3] with a strong emphasis on the generalized approach to inverted pendula systems. All simulation experiments which were included in this paper can be run from the *Demo Simulations* section of the *IPMaC* which contains links to corresponding simulation schemes.

II. Mathematical Modeling and Simulation of the Classical Double Inverted Pendulum

The *classical double inverted pendulum system* is composed of a pair of rigid, homogenous pendulum rods which are interconnected in a joint and one of them is attached to a stable mechanism (cart) which allows for movement alongside a single axis (Fig. 1). It is a typical example of an underactuated system since the number of actuators is lower than the number of system links: the only input (the force $F(t)$ acting upon the cart) is used to control the 3 degrees of freedom of the system: the cart position $\theta_0(t)\ [m]$, the lower pendulum angle $\theta_1(t)\ [rad]$, and upper pendulum angle $\theta_2(t)\ [rad]$.

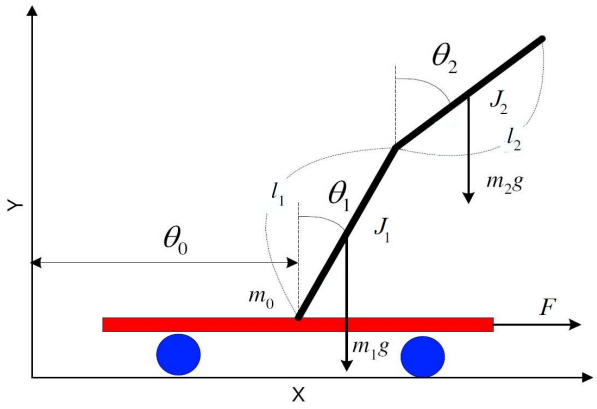

Figure 1. Classical double inverted pendulum system – scheme [4]

A. Automatic Derivation of Motion Equations

Manual, step-by-step derivation of motion equations, done either by Newtonian force summation or by Lagrangian mechanics, is the prevailing approach to inverted pendula modeling which can be found in the accessible works, e.g. [4][5][6]. However, in this paper, the mathematical model of the considered system is generated *automatically* using the *Inverted Pendula Model Equation Derivator*, a MATLAB GUI application

from the *IPMaC* which implements a general procedure that derives the motion equations for a user-chosen type (classical/rotary, single/double) of an inverted pendula system. The procedure, described in detail in [1][2], is an algorithmic implementation of the mathematical model derivation for a generalized (*n-link*) inverted pendula system. Lagrange mechanics is employed since it is well-suited for generalizations of this kind and straightforward to implement with the help of MATLAB's *Symbolic Math Toolbox*.

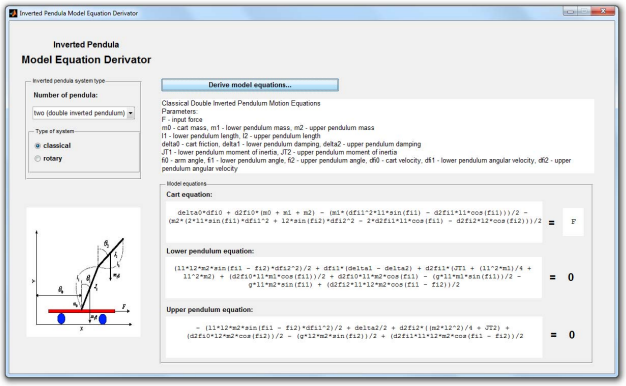

Figure 2. Automatic derivation of the classical double inverted pendulum model equations using the *Inverted Pendula Model Equation Derivator*

As it can be seen in the preview of the *Derivator* window (Fig. 2), the generated model of the classical double inverted pendulum system is composed of three second-order nonlinear differential equations which describe the dynamic behavior of the cart, lower and upper pendulum respectively. After being rewritten into the standard (minimal) ODE form [1] of:

$$\boldsymbol{M}\left(\boldsymbol{\theta}(t)\right)\ddot{\boldsymbol{\theta}}(t)+\boldsymbol{N}\left(\boldsymbol{\theta}(t),\dot{\boldsymbol{\theta}}(t)\right)\dot{\boldsymbol{\theta}}(t)+\boldsymbol{P}\left(\boldsymbol{\theta}(t)\right)=\boldsymbol{V}(t)\,, \quad (1)$$

given that $\boldsymbol{\theta}(t)=\left(\theta_0(t)\;\;\theta_1(t)\;\;\theta_2(t)\right)^T$, the mathematical model of the system assumes the form:

$$\begin{pmatrix} m_0+m_1+m_2 & \left(\frac{1}{2}m_1l_1+m_2l_1\right)\cos\theta_1(t) & \frac{1}{2}m_2l_2\cos\theta_2(t) \\ \left(\frac{1}{2}m_1l_1+m_2l_1\right)\cos\theta_1(t) & J_1+m_2l_1^2 & \frac{1}{2}m_2l_1l_2\cos\left(\theta_1(t)-\theta_2(t)\right) \\ \frac{1}{2}m_2l_2\cos\theta_2(t) & \frac{1}{2}m_2l_1l_2\cos\left(\theta_1(t)-\theta_2(t)\right) & J_2 \end{pmatrix}\begin{pmatrix}\ddot{\theta}_0(t)\\ \ddot{\theta}_1(t)\\ \ddot{\theta}_2(t)\end{pmatrix}+$$
$$+\begin{pmatrix} \delta_0 & -\left(\frac{1}{2}m_1l_1+m_2l_1\right)\dot{\theta}_1(t)\sin\theta_1(t) & \frac{1}{2}m_2l_2\cos\theta_2(t) \\ \frac{1}{2}m_1l_1\cos\theta_1(t) & \delta_1+\delta_2 & -\delta_2 \\ \frac{1}{2}m_2l_2\cos\theta_2(t) & -\frac{1}{2}m_2l_1l_2\dot{\theta}_2(t)\sin\left(\theta_1(t)-\theta_2(t)\right) & \delta_2 \end{pmatrix}\begin{pmatrix}\dot{\theta}_0(t)\\ \dot{\theta}_1(t)\\ \dot{\theta}_2(t)\end{pmatrix}+ \quad (2)$$
$$+\begin{pmatrix} 0 \\ -\left(\frac{1}{2}m_1+m_2\right)gl_1\sin\theta_1(t) \\ -\frac{1}{2}m_2gl_2\sin\theta_2(t) \end{pmatrix}=\begin{pmatrix}F(t)\\0\\0\end{pmatrix}$$

where m_0 is the cart mass, m_1, m_2 are the masses of the lower and upper pendulum respectively, l_1, l_2 are the respective lengths of the pendula, δ_0 is the friction coefficient of the cart against the rail, δ_1, δ_2 are the damping constants in the joints of the pendula, $J_1=\frac{1}{3}m_1l_1^2$, $J_2=\frac{1}{3}m_2l_2^2$ are the moments of inertia of the pendula with respect to the pivot points and $F(t)$ is the force induced on the cart. The derived model (2) will hereafter be referred to as a *force model* of a classical double inverted pendulum system, to distinguish it from a *voltage model* of this system, which will be presented in the section II/C.

B. *Open-Loop Dynamical Analysis*

The *Inverted Pendula Models* sublibrary of the *IPMaC* contains a library block *Classical Double Inverted Pendulum* (*CDIP*) which implements the motion equations (2) derived above. The block is equipped with a dynamic block mask which supports useful features such as editable parameter constants or initial conditions as well as an adjustable number of input and output ports.

The open-loop dynamic behavior of the classical double inverted pendulum system was verified as a response of the *CDIP* block to a force impulse with an amplitude of 0,4N and duration of 1s, starting with all pendula in the upright position. The numeric parameters of the simulation were chosen as follows:

$m_0=0.3kg$, $m_1=m_2=0.275kg$, $l_1=l_2=0.5m$,
$\delta_0=0.3kgs^{-1}$, $\delta_1=0.1kgm^2s^{-1}$, $\delta_2=0.1kgm^2s^{-1}$

The time behavior of the cart position and the freefall and stabilization of the pendula is depicted in Fig. 3 and Fig. 4.

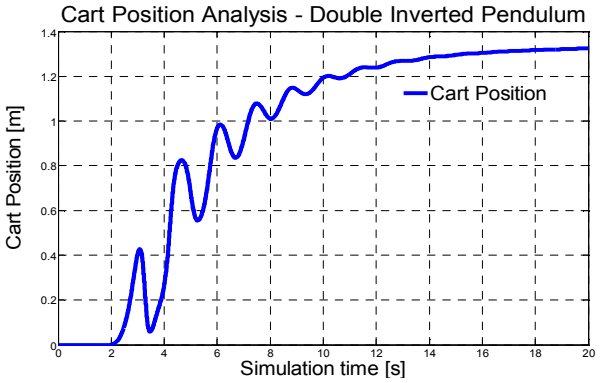

Figure 3. Classical double inverted pendulum (*force model*) – open-loop time behavior of cart position

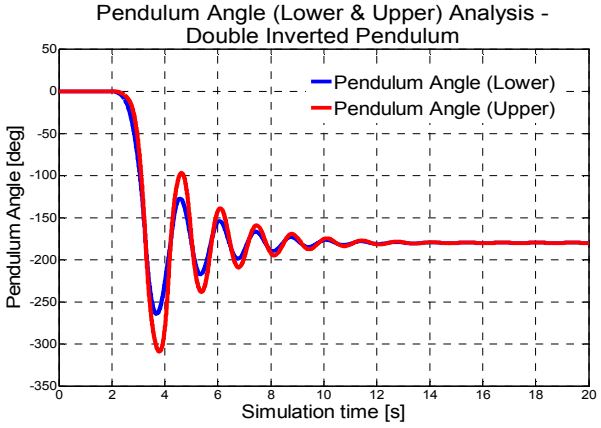

Figure 4. Classical double inverted pendulum (*force model*) – open-loop time behavior of pendula angles

Reasonable behavior of the open-loop response of the *CDIP* simulation model (damped oscillatory transient state, system reaching the stable equilibrium point with all pendula pointing downward, visible backward impact of the pendula on the base) means that the *CDIP* simulation model can be considered accurate enough to serve as a reliable testbed system for linear and nonlinear control algorithms.

C. *Actuating Mechanism Implementation*

As is the case of all inverted pendula systems, the practical use of the classical double inverted pendulum *force model* is limited purely to the simulational environment: we are unable to manually generate a force which would stabilize the pendula in a chosen position. As a result, an electric motor needs to be coupled with the system to act as a mechanism producing the force which actuates both the cart and the attached pendula.

The *Inverted Pendula Motors* sublibrary of the *IPMaC* contains a library block *DC Motor for Inverted Pendula Systems* which implements the mathematical model of a brushed direct-current motor in form of a voltage-to-force conversion relationship, derived in [1] to be:

$$F(t) = \frac{k_m k_g}{R_a r} V_a(t) - \frac{k_m^2 k_g^2}{R_a r^2} \dot{\theta}_0(t) \qquad (3)$$

where $V_a(t)$ is the input voltage applied to the motor, k_m is the motor torque constant, equal in value to the back EMF constant, k_g is the gear ratio, R_a is the armature resistance and r is the radius of the tooth pulley which is coupled to the motor shaft and converts the torque produced by the motor into the linear driving force $F(t)$.

If the DC motor model is appended to an inverted pendulum system (i.e. (3) is substituted into (2)), a *voltage model* of the system is obtained. Fig. 5 and Fig. 6 show the response of the classical double inverted pendulum voltage model to an impulse signal of 5V, lasting 1s. The numeric parameters of the DC motor simulation model were borrowed from the motor featured in the series of popular inverted pendulum laboratory models issued by *Quanser* (*SRV02-Series*), and are specified in [1].

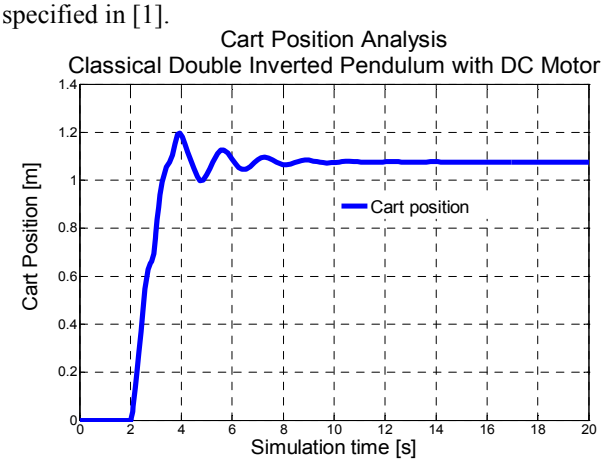

Figure 5. Classical double inverted pendulum (*voltage model*) – open-loop time behavior of cart position

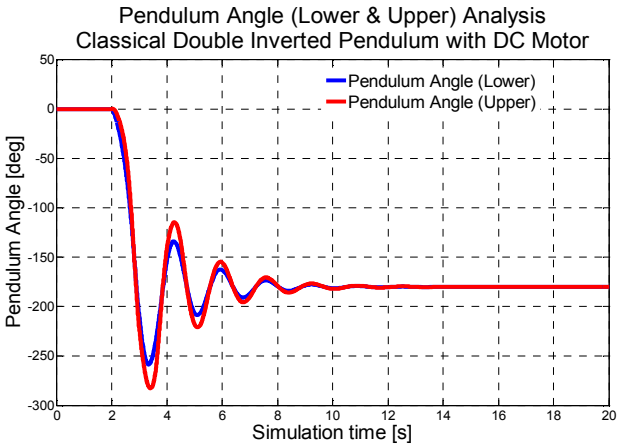

Figure 6. Classical double inverted pendulum (*voltage model*) – open-loop time behavior of pendula angles

For classical inverted pendula systems, the motor-driven inverted pendulum response is much more rigid than that of the force model of the system. This is due to the influence of cart base velocity $\dot{\theta}_0(t)$, stressed by the value of the motor pinion (pulley radius) constant [1].

III. State-Feedback Control Of the Classical Double Inverted Pendulum

The principal control objective was *to stabilize both pendulum links in the vertical upright (inverted) position*, which represents the unstable equilibrium of the system.

Linear state-feedback control was emphasized as the principal control technique because control of several degrees of freedom at once can only be ensured if they are all taken into consideration. Linear approximation is a necessary prerequisite for this approach to control.

A. *Automatic Linear Approximation of the Classical Double Inverted Pendulum System*

If the derived motion equations are rewritten into the (1) form, it is possible to express the classical double inverted pendulum model using the standard nonlinear state-space description in the canonic form:

$$\begin{aligned} \dot{\boldsymbol{x}}(t) &= \boldsymbol{f}\left(\boldsymbol{x}(t), u(t), t\right) \\ \boldsymbol{y}(t) &= \boldsymbol{g}\left(\boldsymbol{x}(t), u(t), t\right) \end{aligned}, \qquad (4)$$

by defining the state vector as $\boldsymbol{x}(t) = \left(\boldsymbol{\theta}(t) \;\; \dot{\boldsymbol{\theta}}(t)\right)$ and isolating the second derivative $\ddot{\boldsymbol{\theta}}(t)$ from (1).

The general procedure implemented by the *Inverted Pendula Model Equation Derivator* uses an assumption which defines the "all-upright" equilibrium as $\boldsymbol{x}(t) = \boldsymbol{x}_S = \boldsymbol{0}^T$. If the input $u(t) = u_S = 0$, then the continuous-time state-space description of the linearized inverted pendula system has the form:

$$\begin{aligned} \dot{\boldsymbol{x}}(t) &= \boldsymbol{A}\boldsymbol{x}(t) + \boldsymbol{b}u(t) \\ \boldsymbol{y}(t) &= \boldsymbol{C}\boldsymbol{x}(t) + du(t) \end{aligned}. \qquad (5)$$

In this paper, the $\boldsymbol{A}$, $\boldsymbol{b}$, $\boldsymbol{C}$, d matrices which make up the linearized state-space model (5) were obtained from the *Inverted Pendula Model Linearizator & Discretizer*, a

MATLAB GUI application which generates the matrices in (5) by expanding (4) into the Taylor series around a given equilibrium point with the higher-order terms neglected (Fig. 7), and also returns the matrices of the discretized state-space model

$$\begin{aligned} \boldsymbol{x}(i+1) &= \boldsymbol{F}\boldsymbol{x}(i) + \boldsymbol{g}u(i) \\ \boldsymbol{y}(i) &= \boldsymbol{C}\boldsymbol{x}(i) + du(i) \end{aligned} \quad . \tag{6}$$

if the sampling period constant has been provided.

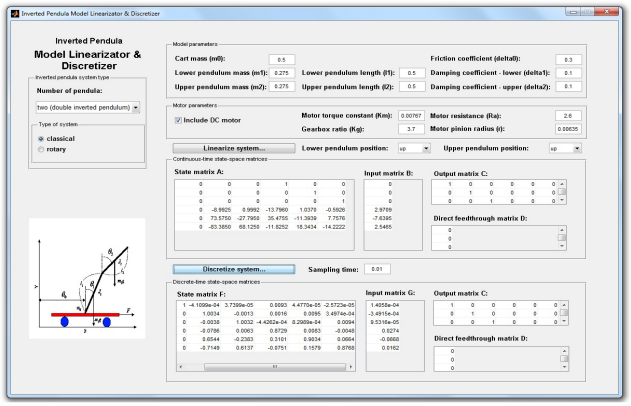

Figure 7. Obtaining the linearized and discretized state-space matrices in the upright position of the classical double inverted pendulum voltage model using the *Inverted Pendula Model Linearizator & Discretizer*

Using the numeric parameters from the open-loop simulations in section II, the continuous-time state-space matrices of the linearized classical double inverted pendulum voltage model were generated as follows:

$$\boldsymbol{A} = \begin{pmatrix} 0 & 0 & 0 & 1 & 0 & 0 \\ 0 & 0 & 0 & 0 & 1 & 0 \\ 0 & 0 & 0 & 0 & 0 & 1 \\ 0 & -8{,}993 & 0{,}992 & -13{,}796 & 1{,}037 & -0.5926 \\ 0 & 73{,}575 & -27{,}79 & 35{,}475 & -11{,}394 & 7{,}758 \\ 0 & -83{,}385 & 68{,}125 & -11{,}825 & 18{,}343 & -14{,}22 \end{pmatrix} \quad \boldsymbol{b} = \begin{pmatrix} 0 \\ 0 \\ 0 \\ 2{,}971 \\ -7{,}64 \\ 2{,}546 \end{pmatrix}$$

The system eigenvalues were computed to be $(0 \quad -31{,}346 \quad -12{,}3629 \quad -3{,}4926 \quad 4{,}0795 \quad 3{,}7099)$, which implies that the linear approximation of the classical double inverted pendulum in the upper equilibrium is an unstable system with first-degree astatism.

The system was next discretized with the sampling period of $T_s = 0{,}01s$ and the following discrete-time state-space matrices were obtained:

$$\boldsymbol{F} = \begin{pmatrix} 1 & -0{,}0004 & 0{,}000 & 0{,}0093 & 0{,}000 & 0{,}000 \\ 0 & 1{,}0034 & -0{,}001 & 0{,}0016 & 0{,}009 & 0{,}0003 \\ 0 & -0{,}0038 & 1{,}0032 & -0{,}0004 & 0{,}0008 & 0{,}0094 \\ 0 & -0{,}0786 & 0{,}0063 & 0{,}873 & 0{,}0083 & -0.0048 \\ 0 & 0{,}6544 & -0{,}238 & 0{,}3101 & 0{,}9034 & 0{,}0664 \\ 0 & -0{,}7149 & 0{,}6137 & -0{,}0751 & 0{,}1579 & 0{,}877 \end{pmatrix} \quad \boldsymbol{g} = \begin{pmatrix} 0{,}0001 \\ -0{,}0003 \\ 0{,}0001 \\ 0{,}0274 \\ -0{,}0668 \\ 0{,}0162 \end{pmatrix}$$

B. State-Feedback Control with a State Estimator

As the principal block of the *Inverted Pendula Control* sublibrary of the *IPMaC*, the *State-Feedback Controller with Feedforward Gain* (*SFCFG*) library block implements the standard state-feedback control law which is calculated either from the continuous-time state-space description:

$$u(t) = u_R(t) + u_{ff}(t) + d_u(t) = -\boldsymbol{k}\boldsymbol{x}(t) + k_{ff}w(t) + d_u(t) \tag{7}$$

or from the discrete-time linear state-space description:

$$u(i) = u_R(i) + u_{ff}(i) + d_u(i) = -\boldsymbol{k}_D x(i) + k_{ffD}w(i) + d_u(i) \tag{8}$$

where $\boldsymbol{k}\,/\,\boldsymbol{k}_D$ is the *feedback gain* which brings the state vector $\boldsymbol{x}(t)\,/\,\boldsymbol{x}(i)$ into the origin of the state space, k_{ff} / k_{ffD} is the *feedforward (setpoint) gain* which makes the output track the reference command and $d_u(t)\,/\,d_u(i)$ is the unmeasured disturbance input [1][2][3]. To match an additional control objective (initial deflection of the pendula, compensation of disturbance signal, tracking a reference position of the cart or a combination of the three), the block's appearance may be adjusted by optional enabling or disabling of the nonzero setpoint input $w(t)\,/\,w(i)$ and the disturbance input $d_u(t)\,/\,d_u(i)$. The method to determine the feedback gain $\boldsymbol{k}\,/\,\boldsymbol{k}_D$ can be selected from between the pole-placement algorithm and the linear quadratic (*LQ*) optimal control method [4][7].

Sometimes measurement limitations make it impossible to retrieve the state-space vector as a whole at every time instant. The *Luenberger Estimator* (*LE*) block provides the controller block with a complete, reconstructed state vector by evaluating a model of the original discrete-time system in the structure:

$$\hat{\boldsymbol{x}}(i+1) = \boldsymbol{F}\hat{\boldsymbol{x}}(i) + \boldsymbol{g}u(i) + \boldsymbol{L}\big(\boldsymbol{y}(i) - \boldsymbol{C}\boldsymbol{x}(i)\big) \tag{9}$$

where $\boldsymbol{L}$ is the estimator gain matrix, $\hat{\boldsymbol{x}}(i)$ is the reconstructed state vector and the estimation error $\tilde{\boldsymbol{x}}(i) = \boldsymbol{x}(i) - \hat{\boldsymbol{x}}(i)$ is being minimized.

Fig. 8 and Fig. 9 depict the results of the feedback control simulation for the classical double inverted pendulum voltage model; *CDIP*, *SFCFG* and *LE* blocks were included in the scheme. The control objective was to maintain the desired cart position while keeping both pendula upright, and the vector of desired closed-loop poles was set to $(-2 \quad -2.5 \quad -4 \quad -5 \quad -3+5i \quad -3-5i)$.

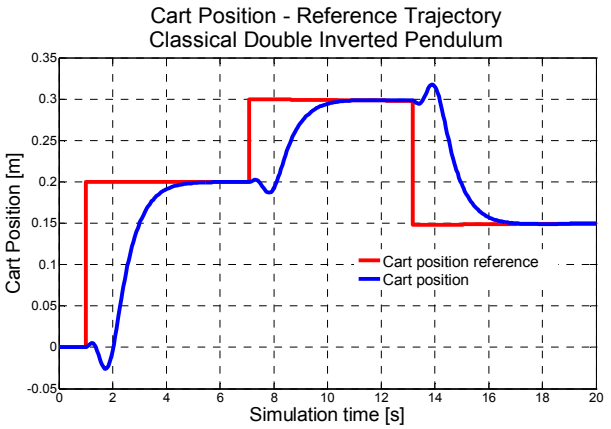

Figure 8. Classical double inverted pendulum: simulation results for pole-placement control – cart position

It was assumed that the cart position and pendula angles would be directly measurable while the velocities would need to be estimated. The vector of estimator poles was set to $\begin{pmatrix} 0.1 & 0.2+0.1i & 0.2-0.1i & 0.25 & 0.3 & 0.35 \end{pmatrix}$.

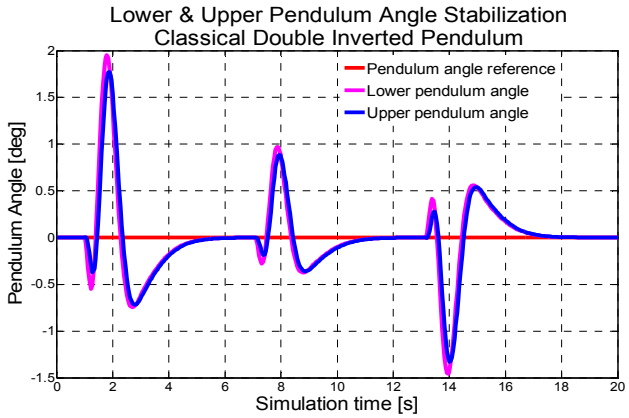

Figure 9. Classical double inverted pendulum: simulation results for pole-placement control – pendulum angles

C. *State-Feedback Control with Permanent Disturbance Compensation*

Applying state-feedback control with feedforward gain on a system is insufficient if the steady-state effect of a permanent disturbance input needs to be compensated. The structure of the *State-Feedback Controller with Summator (SFCS)* block implements a summator term $v(i)$ which sums up all past error values [8]. This ensures that the system output will track the changes in the reference command and eliminate the influence of permanent disturbances. The evaluated control law is specified as

$$u(i) = u_R(i) + u_{ff}(i) + u_S(i) = -\boldsymbol{k}_1 \boldsymbol{x}(i) + k_2 w(i) + v(i) \quad (10)$$

where $w(i)$ is the reference command and $\boldsymbol{k}_1$, k_2 are gain matrices which are computed from a matrix structure derived in [1][8] and implemented into the *SFCS* block.

The control law (8) was verified for the classical double inverted pendulum voltage model and the weight matrices of the standard discrete-time LQ functional

$$J_{LQR}(i) = \sum_{i=0}^{N-1} \boldsymbol{x}^T(i) \boldsymbol{Q} \boldsymbol{x}(i) + u_R^T(i) r u_R(i) \qquad (11)$$

were set to $\boldsymbol{Q} = diag\begin{pmatrix} 500 & 10 & 20 & 20 & 10 & 10 \end{pmatrix}$, $r = 1$. The results were compared to those of a conventional state-feedback controller using the same values of weight matrices. A constant disturbance input (10V for the first controller, 1V for the second) was present in both simulations. To compensate for measurement limitations, the *LE* block was included in both schemes, with the estimator poles set to the same values as in section III/B.

As it can be seen in Fig. 10 – Fig. 12, the conventional LQR controller fails to track the reference trajectory without producing steady-state error, but the permanent disturbances are successfully compensated by a LQR algorithm with a summator included in the control structure.

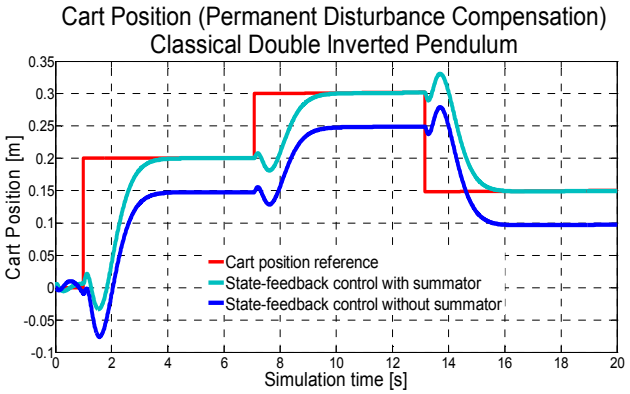

Figure 10. Classical double inverted pendulum: simulation results for LQR control with a summator – cart position

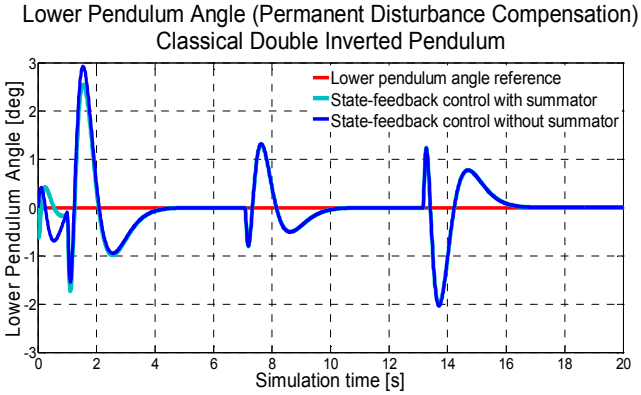

Figure 11. Classical double inverted pendulum: simulation results for LQR control with a summator – lower pendulum angle

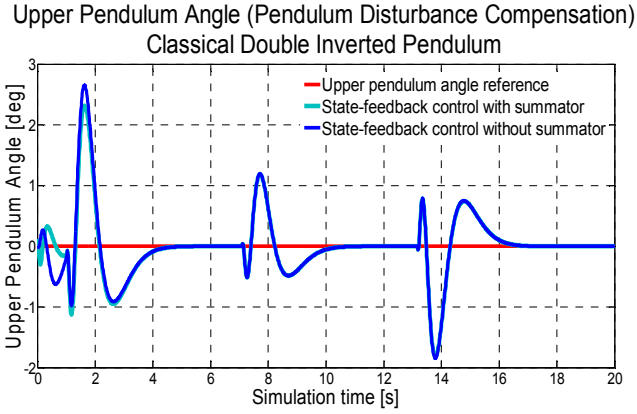

Figure 12. Classical double inverted pendulum: simulation results for LQR control with a summator – upper pendulum angle

IV. Conclusion

The purpose of this paper was to present a comprehensive approach to the modeling and control of the classical double inverted pendulum system. *Inverted Pendula Modeling and Control,* a custom-designed *Simulink* block library developed by the authors of the paper, was used as a software framework for all covered issues which included model derivation and open-loop analysis, linearization and state-feedback control algorithm design.

The library provided suitable function blocks to support every step of the process (e.g. a pre-prepared simulation model of the classical double inverted pendulum system or a detailed state-feedback controller block) as well as several innovative applications with graphical user interface. One of these was used to derive the mathematical model for the selected inverted pendulum system in form of symbolic equations of motion, and the other performed the automatic linear transformation of the system in a selected equilibrium point. In these applications, great practical potential of the symbolic mathematical software was demonstrated.

The *IPMaC* block library enhances the capabilities of the *MATLAB/Simulink* program environment by providing means for modeling and control of an important class of nonlinear mechanical systems. It can therefore be considered as a meaningful contribution to modeling and control education at technical universities.

ACKNOWLEDGMENT

This work has been supported by the Scientific Grant Agency of Slovak Republic under project Vega No.1/0286/11 Dynamic Hybrid Architectures of the Multiagent Network Control Systems (50%). This work is also the result of the project implementation Development of the Center of Information and Communication Technologies for Knowledge Systems (project number: 26220120030) supported by the Research & Development Operational Program funded by the ERDF (50%).

REFERENCES

[1] S. Jadlovská, *Modeling and Optimal Control of Inverted Pendula Systems*, Diploma (Master) Thesis. Supervisor: prof. Ing. Ján Sarnovský, CSc.. Košice: Technical University of Košice, Faculty of Electrical Engineering a Informatics, 2011.

[2] S. Jadlovská, A. Jadlovská, "Inverted Pendula Simulation and Modeling – a Generalized Approach," *Proceedings of the 9th International Scientific – Technical Conference on Process Control*, June 7-10, 2010, University of Pardubice, Czech Republic, ISBN 978-80-7399-951-3.

[3] S. Jadlovská, J. Sarnovský, "An extended Simulink library for modeling and control of inverted pendula systems," *Proceedings of the International Scientific Conference - Technical Computing*, *2011*, in press.

[4] A. Bogdanov, *Optimal Control of a Double Inverted Pendulum on a Cart*, Technical Report CSE-04-006, OGI School of Science and Engineering, OHSU, 2004.

[5] M. Demirci, "Design of Feedback Controllers for a Linear System with Applications to Control of a Double Inverted Pendulum," *International Journal of Computational Cognition*, Vol. 2, No. 1, p. 65-84, 2004.

[6] M. Schlegel, J. Mešťánek, "Limitations on the Inverted Pendula Stabilizability According to Sensor Placement," *Proceedings of the 16th International Conference on Process Control,* June 11-14, 2007, Štrbské Pleso, Slovakia.

[7] J. Sarnovský – A. Jadlovská – P. Kica, *Optimal and Adaptive Systems Theory* [Teória optimálnych a adaptívnych systémov], Košice: ELFA s r.o., 2005, ISBN 80-8086-020-3.

[8] O. Modrlák, *Automatic Control Theory, vol. 1 – Basic State-Space Analysis and Synthesis (Study Material)* [Teorie automatického řízení I. - Základy analýzy a syntézy ve stavovém prostoru (Studijní materiály)], Liberec: Technical University of Liberec, 2002.